

# ChemComm

Chemical Communications

Accepted Manuscript

This article can be cited before page numbers have been issued, to do this please use: E. Zars, L. Pick, A. Kankanamge, M. Gau, K. Meyer and D. J. Mindiola, *Chem. Commun.*, 2024, DOI: 10.1039/D4CC04127E.



This is an Accepted Manuscript, which has been through the Royal Society of Chemistry peer review process and has been accepted for publication.

Accepted Manuscripts are published online shortly after acceptance, before technical editing, formatting and proof reading. Using this free service, authors can make their results available to the community, in citable form, before we publish the edited article. We will replace this Accepted Manuscript with the edited and formatted Advance Article as soon as it is available.

You can find more information about Accepted Manuscripts in the [Information for Authors](#).

Please note that technical editing may introduce minor changes to the text and/or graphics, which may alter content. The journal's standard [Terms & Conditions](#) and the [Ethical guidelines](#) still apply. In no event shall the Royal Society of Chemistry be held responsible for any errors or omissions in this Accepted Manuscript or any consequences arising from the use of any information it contains.

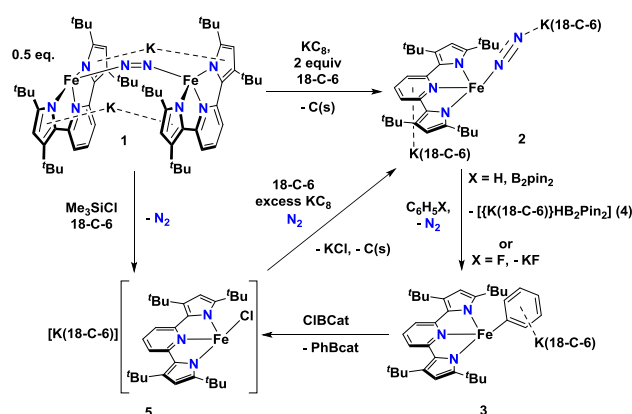
## COMMUNICATION

**C<sub>sp2</sub>-H/F bond activation and borylation with low valent iron**Ethan Zars,<sup>a</sup> Lisa Pick,<sup>b</sup> Achala Kankanamge,<sup>a</sup> Michael Gau,<sup>a</sup> Karsten Meyer,<sup>\*,b</sup> and Daniel J. Mindiola<sup>\*,a</sup>Received 00th January 20xx,  
Accepted 00th January 20xx

DOI: 10.1039/x0xx00000x

Reduction of [K<sub>2</sub>{(t<sup>Bu</sup>pyrr<sub>2</sub>pyr)Fe}<sub>2</sub>(μ-N<sub>2</sub>)] (1) with two equiv of KC<sub>8</sub> in the presence of crown-ether 18-C-6 yields the N<sub>2</sub> adduct [{K(18-C-6)}<sub>2</sub>{(t<sup>Bu</sup>pyrr<sub>2</sub>pyr)Fe(N<sub>2</sub>)}] (2). Complex 2 heterolytically splits the C<sub>sp2</sub>-H bond of benzene to form [{K(18-C-6)}{(t<sup>Bu</sup>pyrr<sub>2</sub>pyr)Fe(C<sub>6</sub>H<sub>5</sub>)}] (3), whereby usage of a diboron B<sub>2</sub>pin<sub>2</sub> promotes hydride elimination to form the salt [K(18-C-6)HB<sub>2</sub>pin<sub>2</sub>] (4). Similarly, 3 can also be formed by cleavage of the C-F bond of fluorobenzene. Reaction of 3 with ClBcat yields [K(18-C-6)(thf)<sub>2</sub>]{(t<sup>Bu</sup>pyrr<sub>2</sub>pyr)FeCl} (5) and PhBcat and the former can be reduced to 2 to complete a synthetic cycle for heterolytic benzene C-H activation and borylation.

The activation and functionalization of C-H bonds is a crucial step toward converting an unreactive and abundant substrate into more reactive or synthetically versatile functionalities.<sup>1</sup> Much of the early literature on C-H activation focuses on the oxidative addition of C-H bonds at low valent precious metals.<sup>2</sup> This research was performed in the context of cross-coupling reactions which typically go through catalytic cycles consisting of oxidative addition, transmetalation, and reductive elimination.<sup>3</sup> A particularly useful target for C-H functionalization would be the generation of C-B bonds due to their prevalence in Suzuki-Miyaura cross coupling reactions.<sup>4</sup> While C-H activation is usually accomplished with precious metals, there is precedent for this reaction at low valent iron,<sup>5</sup> which is the most abundant metal in Earth's crust.<sup>6</sup> To this end, borylation of aryl C<sub>sp2</sub>-H bonds by photolysis of an iron boryl species has been reported,<sup>7</sup> with more recent studies expanding this work to catalytic processes for C-H borylation.<sup>8</sup> While mechanistic studies for arene C-H borylation reactions have been studied in detail for first row transition metals such as Co,<sup>9</sup> similar studies clearly showing the bond forming and breaking



**Scheme 1.** Reaction scheme outlining formation and reactions of [{K(18-C-6)}<sub>2</sub>{(t<sup>Bu</sup>pyrr<sub>2</sub>pyr)Fe(N<sub>2</sub>)}] (2).

processes at the Fe center have been exceptionally rare.<sup>5e,7b,7c,8a,8j,10</sup>

In this contribution, we show how a formally Fe(0) and mononuclear Fe dinitrogen complex [{K(18-C-6)}<sub>2</sub>{(t<sup>Bu</sup>pyrr<sub>2</sub>pyr)Fe(N<sub>2</sub>)}] (2) (t<sup>Bu</sup>pyrr<sub>2</sub>pyr<sup>2-</sup> = 3,5-t<sup>Bu</sup><sub>2</sub>-bis(pyrr<sub>2</sub>pyr)pyridine; 18-C-6 = 18-crown-6) can activate the C<sub>sp2</sub>-H bond of benzene (and the C-F bond of fluorobenzene) at room temperature to yield the iron phenyl complex [{K(18-C-6)}{(t<sup>Bu</sup>pyrr<sub>2</sub>pyr)Fe(C<sub>6</sub>H<sub>5</sub>)}] (3). We propose the C-H activation process to be heterolytic in nature by trapping KH with B<sub>2</sub>pin<sub>2</sub> (pin = pinacolato) to form the adduct [K(18-C-6)HB<sub>2</sub>pin<sub>2</sub>] (4). The aryl ligand from 3 can be transmetalated using ClBcat (cat = catecholato) to yield the discrete salt [{K(18-C-6)(thf)<sub>2</sub>}{(t<sup>Bu</sup>pyrr<sub>2</sub>pyr)FeCl}] (5) along with the borane PhBcat (6). Finally, we show how 5 can be reduced to 2 to close a synthetic cycle for room temperature C<sub>sp2</sub>-X bond activation and borylation (Scheme 1).

We have previously shown that reduction of the ferrous precursor [(t<sup>Bu</sup>pyrr<sub>2</sub>pyr)Fe(OEt<sub>2</sub>)]<sup>11</sup> with one equiv of KC<sub>8</sub> yields the formally Fe<sup>I</sup> end-on and bridging N<sub>2</sub> complex [K<sub>2</sub>{(t<sup>Bu</sup>pyrr<sub>2</sub>pyr)Fe}<sub>2</sub>(μ-N<sub>2</sub>)] (1) in which the N<sub>2</sub> ligand bridging the two Fe centers is topologically nonlinear.<sup>12</sup> Such a geometry

<sup>a</sup> Department of Chemistry, University of Pennsylvania, 231 S 34th St, Philadelphia, PA, USA 19104.

<sup>b</sup> Department of Chemistry & Pharmacy, Inorganic Chemistry, Friedrich-Alexander-Universität Erlangen - Nürnberg (FAU) 91058 Erlangen, Germany

† Electronic Supplementary Information (ESI) available: [ESI contains complete experimental details and spectral data]. See DOI: 10.1039/x0xx00000x

\*Corresponding Authors: karsten.meyer@fau.de; mindiola@sas.upenn.edu



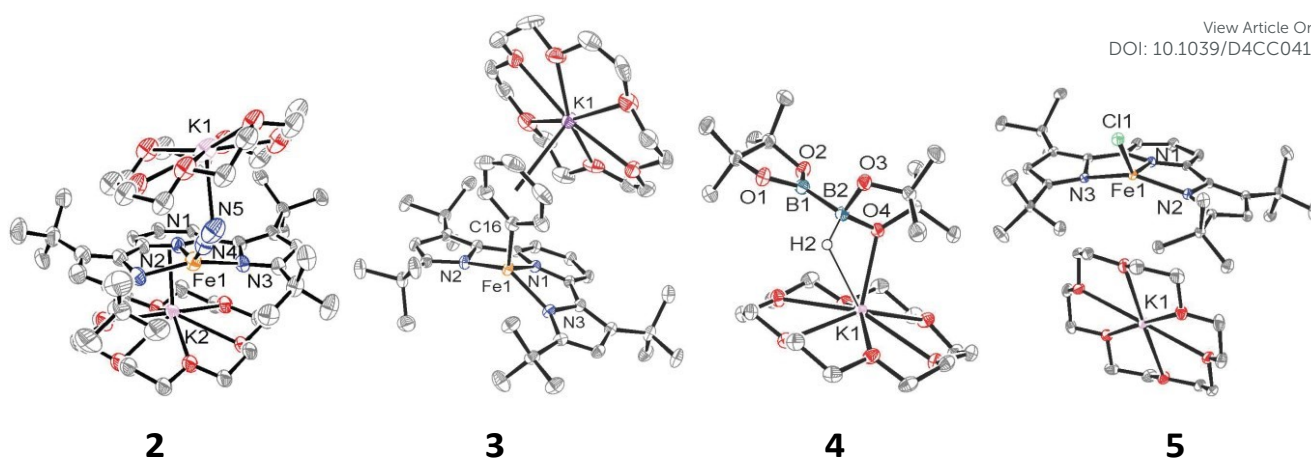


**Figure 1.** ORTEP *sc*-XRD structures of complexes **2**, **3**, **4**, and **5** at 50% probability level. Residual solvent molecules and H atoms (with the exception of the hydride in compound **4**) have been omitted for clarity. Coordinated thf molecules coordinated to K in compound **5** have been also omitted.

is retained upon further reduction to the formally Fe<sup>0</sup> complex  $[\{K_2(18-C-6)\}(\text{t}^{\text{Bu}}\text{pyrr}_2\text{pyr})\text{Fe}_2(\mu\text{-N}_2)]$  or via oxidative substitution of N<sub>2</sub> with chalcogenides.<sup>13</sup> The full extent of low-valent iron chemistry using the  $\text{t}^{\text{Bu}}\text{pyrr}_2\text{pyr}$  ligand platform, especially as it pertains to mononuclear complexes, has so far been unexplored. Treatment of **1** with four equivalents of 18-C-6 and two equivalents of K<sub>2</sub>C<sub>8</sub> in toluene at room temperature resulted in the initial formation of a brown residue. Allowing the reaction to stir for an additional hour at room temperature led to the conversion of the brown residue to a dark purple solution. After filtration and concentration *in vacuo*, the solution was cooled to -35 °C overnight to afford  $[\{K(18-C-6)\}_2(\text{t}^{\text{Bu}}\text{pyrr}_2\text{pyr})\text{Fe}(\text{N}_2)]$  (**2**) which could be isolated in 79% yield as black crystals (Scheme 1, Fig 1). The <sup>1</sup>H NMR spectrum of **2** shows seven paramagnetically broadened and shifted resonances indicative of a C<sub>s</sub> symmetric system (Fig S1). A single crystal X-Ray diffraction study (*sc*-XRD) of **2** shows a  $(\text{t}^{\text{Bu}}\text{pyrr}_2\text{pyr})\text{Fe}$  scaffold with a terminal N<sub>2</sub> ligand occupying the fourth coordination site and capped by a  $\{K(18-C-6)\}^+$  unit. The second  $\{K(18-C-6)\}^+$  is coordinated to the pyridyl portion of the meridional ligand. The geometry at the formally zero valent Fe center in **2** can best be described as seesaw with a  $\langle\text{N}_{\text{pyr}}\text{-Fe-N}_2\rangle$  angle of 140.7(2)° and a  $\tau_4$  value of 0.51. The N<sub>2</sub> ligand has an N-N bond length of 1.147(6) Å and a signature stretch at 1851 cm<sup>-1</sup> in the IR spectrum (Figure S21) implying significant activation of the N<sub>2</sub> ligand when compared to its free form (1.0975 Å, 2331 cm<sup>-1</sup>).<sup>14</sup> The low energy vibration and elongated N-N bond for the N<sub>2</sub> ligand implies not only the metal ion but the N<sub>2</sub> ligand to be the likely locus of reduction.<sup>15</sup> While we cannot determine the Fe oxidation state of **2** with complete certainty, a significantly shortened Fe-N<sub>2</sub> bond length of 1.775(4) Å and solution state magnetic moment of 4.1  $\mu_B$  measured by Evans Method in C<sub>6</sub>D<sub>6</sub>, which is above the expectation value for a S = 1 system, implies contribution of a Fe(I) atom and N<sub>2</sub>-centered radical to the complicated electronic structure. In contrast to the bridging nature of  $[\{K_2(18-C-6)\}(\text{t}^{\text{Bu}}\text{pyrr}_2\text{pyr})\text{Fe}_2(\mu\text{-N}_2)]$ , we propose the mononuclear structure of **2** to derive from the addition of more equivalents of 18-crown-6.

Interested in the oxidative chemistry of **2**, we treated this species with one equivalent of bispinacolato diboron (B<sub>2</sub>pin<sub>2</sub>) in benzene expecting to observe reductive cleavage of the B-B bond. However, upon addition of the B<sub>2</sub>pin<sub>2</sub> the reaction mixture gradually changed color from dark purple to red, and over 16 hours there is deposition of red crystals. A *sc*-XRD study on single crystals isolated from the reaction mixture confirms the structure to be instead the discrete phenyl salt  $[\{K(18-C-6)\}(\text{t}^{\text{Bu}}\text{pyrr}_2\text{pyr})\text{Fe}(\text{C}_6\text{H}_5)]$  (**3**) isolated in 61% yield. The solid-state structure of **3** shows a formally Fe<sup>II</sup> ion with an Fe-C bond length of 2.068(1) Å resulting from benzene activation. The  $\langle\text{N}_{\text{pyr}}\text{-Fe-C}_{\text{Ar}}\rangle$  angle is 123.88(5)° and the geometric index value of  $\tau_4 = 0.74$  is consistent with a distorted *cis*-divacant octahedral coordination geometry. A <sup>1</sup>H NMR spectroscopic study of these crystals in thf-*d*<sub>3</sub> shows 9 paramagnetically shifted and broadened resonances showing preservation of a C<sub>s</sub> symmetric system in solution (Fig S2). A room temperature solution state magnetic moment of 4.8  $\mu_B$  determined by Evans method is close to the spin only value for an S = 2 system in accord with a high spin Fe<sup>II</sup> ion in **3**. Examination of the supernatant from the reaction between **2** and B<sub>2</sub>Pin<sub>2</sub> by <sup>11</sup>B NMR spectroscopy in thf-*d*<sub>3</sub> revealed two resonances at 30.97 ppm and 5.91 ppm (Fig S9). Resonances in these positions can be attributed to one trigonal planar and one pyramidal B atom as demonstrated by Marder and coworkers in a series of  $[\{K(18\text{-crown-6})\}\text{XB}_2\text{Pin}_2]$  discrete salt molecules where X = O<sup>t</sup>Bu, OMe, and F.<sup>16</sup> The B-containing molecule could be crystallized out of a concentrated thf solution at -35 °C and its structure determined to be  $[\{K(18\text{-crown-6})\}\text{HB}_2\text{Pin}_2]$  (**4**). A *sc*-XRD structure of **4** clearly shows a HB<sub>2</sub>Pin<sub>2</sub> core with two distinctly different B centers as well as a  $[K(18-C-6)]^+$  counter ion interacting with the hydride and nearby pinacolato oxygen. <sup>11</sup>B NMR spectroscopy of the crystals also showed, as expected, two resonances, albeit at slightly different chemical shifts (Fig S8) when compared to the crude material. We attribute this discrepancy to the lack of paramagnetic impurities in the crystalline material contributing to a noncontact paramagnetic shift.<sup>17</sup> Transfer of a hydrogen atom to a borane has been reported before in the context of C-H



activation at low valent iron centers, but diboron reagents have not been used to sponge out the hydride most likely stemming from heterolytic C–H bond cleavage.<sup>5e,5g</sup> Using other hydride acceptors such as imines and nitriles or other Lewis acids such as  $B(C_6F_5)_3$  did not result in the formation of **3** (Figs S13–S17). We found that complex **3** could also be generated by reaction of **2** with fluorobenzene at room temperature (Scheme 1) in a manner similar to Holland's work using low valent Co complexes,<sup>18</sup> albeit the reaction was not quantitative thus resulting in formation of other intractable materials (Fig S10). Selective C–F bond activation is rare<sup>19</sup> and C–F bonds are known to be stable toward catalytic C–H borylation protocols.<sup>8a,8c,8h,9c</sup> Having demonstrated that **2** could undergo C–H activation of benzene we next turned to delivering or functionalizing the phenyl moiety of **3**. Accordingly, treatment of **3** with one equivalent of ClBcat in *thf-d*<sub>8</sub> results in a new paramagnetic molecule when judged by <sup>1</sup>H NMR spectroscopy. Likewise, <sup>1</sup>H and <sup>11</sup>B NMR spectroscopy confirm that a second, diamagnetic species was formed, namely PhBCat (Fig S19, <sup>11</sup>B NMR  $\delta = 32.6$ ).<sup>20</sup> The paramagnetic product was identified to be  $[K(18-C-6)(thf)_2]([t^Bu-pyrr_2pyr]FeCl)$  (**5**) using a combination of <sup>1</sup>H NMR, *sc*-XRD, solution magnetic susceptibility studies, as well as by an independent synthesis in 92% isolated yield via addition of 2 equivalents of Me<sub>3</sub>SiCl to the N<sub>2</sub> precursor **1** (Scheme 1). A <sup>1</sup>H NMR spectrum in *thf-d*<sub>8</sub> is consistent with a plane of symmetry bisecting **5** given the observation of seven paramagnetically shifted and broadened resonances (Fig S3). A *sc*-XRD study on **5** shows the (*t*<sup>Bu</sup>pyrr<sub>2</sub>pyr)Fe core with a chloride ligand occupying the fourth coordination site and  $[K(18-crown-6)(thf)_2]^+$  in the unit cell but not interacting with the iron complex. The Fe–Cl bond length is 2.2914(5) Å which is longer than the Fe–Cl bond length of 2.1883(9) Å in the neutral ferric congener  $[([t^Bu-pyrr_2pyr]FeCl)]$ .<sup>11</sup> In the structure of **5** the  $\langle N_{pyr}-Fe-Cl$  angle is 135.34(3)° and the geometric index  $\tau_4$  value is 0.60 which makes this geometry best described as seesaw. A solution state magnetic moment of **5** determined by Evans method is 5.4  $\mu_B$  and is consistent with an  $S = 2$  system.

In the interest investigating the electronic structures of these mononuclear formally Fe<sup>II</sup> ate complexes (**3** and **5**), <sup>57</sup>Fe Mössbauer spectroscopy and DC SQUID magnetometry measurements were performed on complex **5** as a representative example of this new class of compounds (Fig 2). <sup>57</sup>Fe Mössbauer spectroscopy of **5** at 77 K shows a quadrupole doublet with an isomer shift of  $\delta = 0.82$  mm·s<sup>-1</sup>, a quadrupole splitting of  $\Delta E_Q = 1.02$  mm·s<sup>-1</sup>, and a linewidth of  $\Gamma_{FWHM} = 0.32$  mm·s<sup>-1</sup>. These values are consistent with a  $S = 2$  Fe<sup>II</sup> ion on the *t*<sup>Bu</sup>pyrr<sub>2</sub>pyr ligand platform.<sup>11,13,21</sup> This spin state was confirmed by a DC SQUID magnetometry study which showed a field-independent magnetic moment of 5.28  $\mu_B$  (averaged between two samples) at 300 K. Unfortunately, due to difficulties in scaling up the synthesis of **3**, we were unable to collect reliable <sup>57</sup>Fe Mössbauer spectroscopy and DC SQUID magnetometry measurements on this complex. We can, however, be reasonably confident in our assignment of its oxidation and spin state as  $S = 2$  Fe<sup>II</sup> due to its solution state magnetic moment of 4.8  $\mu_B$  and similarities with **5** in its electronic absorption spectrum (Figs S22, S23).

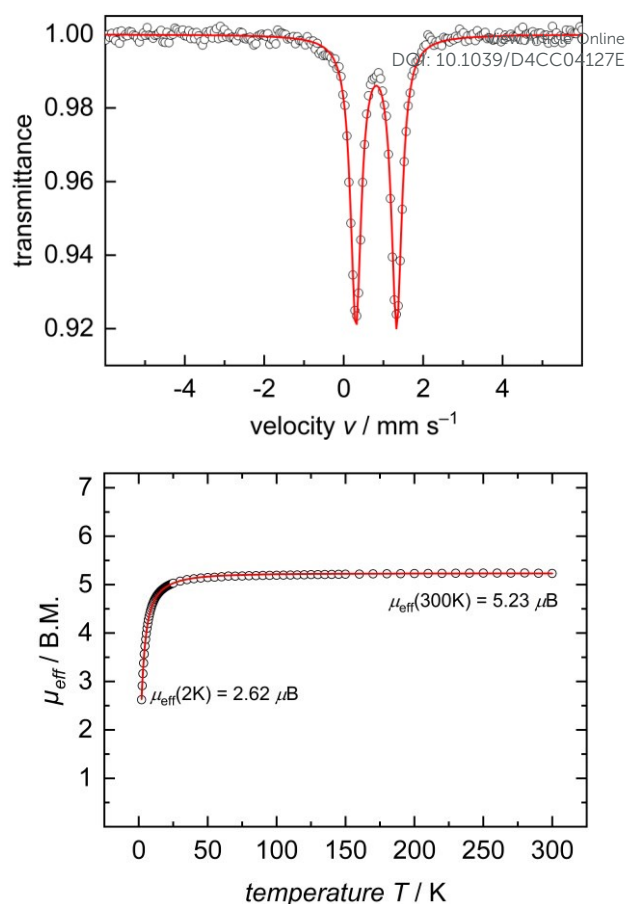


**Fig 2. (top)** Zero-field <sup>57</sup>Fe-Mössbauer spectrum of **5** (solid state, 77 K). Measured data was fit with parameters  $\delta = 0.82$  mm·s<sup>-1</sup>,  $\Delta E_Q = 1.02$  mm·s<sup>-1</sup>, and  $\Gamma_{FWHM} = 0.32$  mm·s<sup>-1</sup>. **(bottom)** Temperature-dependent SQUID DC field measurement of a powdered sample of **5** recorded from 2 to 300 K with an applied magnetic field of 1 T. Measured data was fit with parameters  $S = 2$ ,  $TIP = 1023 \times 10^{-6}$  emu,  $|D| = 12$  cm<sup>-1</sup>,  $E/D = 0.14$ , and  $g_{av} = 2.14$ .

When complex **5** is reduced with an excess of KC<sub>8</sub> and one equivalent of 18-C-6 under an N<sub>2</sub> atmosphere, a gradual color change from red to dark purple is observed. Filtering the solution after one hour of reaction time and crystallization out of a concentrated toluene solution yields small black crystals that were identified as complex **2** by <sup>1</sup>H NMR spectroscopy (Fig S20), thus completing a synthetic cycle of benzene activation and borylation involving the Fe<sup>0</sup>/Fe<sup>II</sup> couple. Future work will involve attempts at rendering this system catalytic as well as expanding the substrate scope with the aim of site-selective C–H bond activation.

This work was supported by the U.S. Department of Energy, Office of Basic Energy Sciences (DOE-BES-DESC0023340) and the University of Pennsylvania (UPenn, DJM), and the Alexander von Humboldt Foundation (KM and DJM). A.K. thanks the Vagelos Integrated Program in Energy Research at UPenn for support.

## Author Contributions





EZ synthesized the complexes, and wrote part of the manuscript. LP collected and analysed the Mössbauer and SQUID data. AK assisted with the synthesis of complexes. MRG solved and curated the crystal structures. KM and DJM provided funding and equipment for the project and helped compose the manuscript.

## Data Availability

Data for this article including full synthetic procedures and characterization are available in the Supplementary Information at <https://doi.org/DOI>.

## Conflicts of interest

There are no conflicts to declare

## References

- (a) S. K. Bose, L. Mao, L. Kuehn, U. Radius, J. Nekvinda, W. L. Santos, S. A. Westcott, P. G. Steel and T. B. Marder, *Chem. Rev.*, 2021, **121**, 13238–13341. (b) I. F. Yu, J. W. Wilson and J. F. Hartwig, *Chem. Rev.*, 2023, **123**, 11619–11663. (c) R. Arevalo and P. J. Chirik, *J. Am. Chem. Soc.*, 2019, **141**, 9106–9123.
- (a) M. Lersch and M. Tilset, *Chem. Rev.*, 2005, **105**, 2471–2526. (b) J. A. Labinger and J. E. Bercaw, *Nature*, 2002, **417**, 507–514. (c) B. A. Arndtsen, R. G. Bergman, T. A. Mobley and T. H. Peterson, *Acc. Chem. Res.*, 1995, **28**, 154–162. (d) A. E. Shilov and G. B. Shul'pin, *Chem. Rev.*, 1997, **97**, 2879–2932. (e) R. H. Crabtree, *J. Chem. Soc., Dalton Trans.*, 2001, 2437–2450.
- (a) K. C. Nicolaou, P. G. Bulger and D. Sarlah, *Angew. Chem., Int. Ed.*, 2005, **44**, 4442–4489. (b) J. K. Stille, *Angew. Chem., Int. Ed. Engl.*, 1986, **25**, 508–524. (c) X. Chen, K. M. Engle, D. H. Wang and Y. Jin-Quan, *Angew. Chem., Int. Ed.*, 2009, **48**, 5094–5115.
- Norio. Miyaura and Akira. Suzuki, *Chem. Rev.*, 1995, **95**, 2457–2483.
- (a) S. Camadanli, R. Beck, U. Flörke and H.-F. Klein, *Organometallics*, 2009, **28**, 2300–2310. (b) M. V Baker and L. D. Field, *J. Am. Chem. Soc.*, 1987, **109**, 2825–2826. (c) L. D. Field, R. W. Guest and P. Turner, *Inorg. Chem.*, 2010, **49**, 9086–9093. (d) S. Camadanli, R. Beck, U. Flörke and H.-F. Klein, *Organometallics*, 2009, **28**, 2300–2310. (e) A. Casitas, H. Krause, S. Lutz, R. Goddard, E. Bill and A. Fürstner, *Organometallics*, 2018, **37**, 729–739. (f) S. D. Ittel, C. A. Tolman, A. D. English and J. P. Jesson, *J. Am. Chem. Soc.*, 1976, **98**, 6073–6075. (g) S. F. McWilliams, D. L. J. Broere, C. J. V Halliday, S. M. Bhutto, B. Q. Mercado and P. L. Holland, *Nature*, 2020, **584**, 221–226. (h) W. D. Jones, G. P. Foster and J. M. Putinas, *J. Am. Chem. Soc.*, 1987, **109**, 5047–5048. (i) M. K. Whittlesey, R. J. Mawby, R. Osman, R. N. Perutz, L. D. Field, M. P. Wilkinson and M. W. George, *J. Am. Chem. Soc.*, 1993, **115**, 8627–8637. (j) C. A. Tolman, S. D. Ittel, A. D. English and J. P. Jesson, *J. Am. Chem. Soc.*, 1979, **101**, 1742–1751. (k) A. K. Hickey, S. A. Lutz, C.-H. Chen and J. M. Smith, *Chem. Commun.*, 2017, **53**, 1245–1248.
- W. M. Haynes, D. R. Lide and T. J. Bruno, Eds., CRC Press, Boca Raton, FL, 97th edn., 2016, p. 19.
- (a) K. M. Waltz, X. He, C. Muhoro and J. F. Hartwig, *J. Am. Chem. Soc.*, 1995, **117**, 11357–11358. (b) T. J. Mazzacano and N. P. Mankad, *Chem. Commun.*, 2015, **51**, 5379–5382. (c) K. M. Waltz, C. N. Muhoro and J. F. Hartwig, *Organometallics*, 1999, **18**, 3383–3393.
- (a) L. Britton, J. H. Docherty, G. S. Nichol, A. P. Dominey and S. P. Thomas, *Chin. J. Chem.*, 2022, **40**, 2875–2881. (b) T. Dombray, C. G. Werncke, S. Jiang, M. Grellier, L. Vendier, S. Bontemps, J.-B. Sortais, S. Sabo-Etienne and C. Darcel, *J. Am. Chem. Soc.*, 2015, **137**, 4062–4065. (c) M. Kamitani, H. Kusaka and H. Yuge, *Chem. Lett.*, 2019, **48**, 898–901. (d) J.-L. Tu, A.-M. Hu, L. Guo and W. Xia, *J. Am. Chem. Soc.*, 2023, **145**, 7600–7611. (e) T. J. Mazzacano and N. P. Mankad, *J. Am. Chem. Soc.*, 2013, **135**, 17258–17261. (f) G. Yan, Y. Jiang, C. Kuang, S. Wang, H. Liu, Y. Zhang and J. Wang, *Chem. Commun.*, 2010, **46**, 3170–3172. (g) T. Kato, S. Kuriyama, K. Nakajima and Y. Nishibayashi, *Chem. Asian J.*, 2019, **14**, 2097–2101. (h) H. Lee, T. He and S. P. Cook, *Org. Lett.*, 2023, **25**, 1–4. (i) M. Kamitani, *Chem. Commun.*, 2021, **57**, 13246–13258. (j) T. Hatanaka, Y. Ohki and K. Tatsumi, *Chem. Asian J.*, 2010, **5**, 1657–1666.
- (a) J. V. Obligation, S. P. Semproni, I. Pappas and P. J. Chirik, *J. Am. Chem. Soc.*, 2016, **138**, 10645–10653. (b) J. V. Obligation, S. P. Semproni and P. J. Chirik, *J. Am. Chem. Soc.*, 2014, **136**, 4133–4136. (c) T. P. Pabst and P. J. Chirik, *J. Am. Chem. Soc.*, 2022, **144**, 6465–6474.
- S. R. Parmelee, T. J. Mazzacano, Y. Zhu, N. P. Mankad and J. A. Keith, *ACS Catal.*, 2015, **5**, 3689–3699.
- K. Searles, S. Fortier, M. M. Khusniyarov, P. J. Carroll, J. Sutter, K. Meyer, D. J. Mindiola and K. G. Caulton, *Angew. Chem., Int. Ed.*, 2014, **53**, 14139–14143.
- D. Sorsche, M. E. Miehlich, K. Searles, G. Gouget, E. M. Zolnhofer, S. Fortier, C.-H. Chen, M. Gau, P. J. Carroll, C. B. Murray, K. G. Caulton, M. M. Khusniyarov, K. Meyer and D. J. Mindiola, *J. Am. Chem. Soc.*, 2020, **142**, 8147–8159.
- E. Zars, L. Gravogl, M. R. Gau, P. J. Carroll, K. Meyer and D. J. Mindiola, *Chem. Sci.*, 2023, **14**, 6770–6779.
- (a) N. Hazari, *Chem. Soc. Rev.*, 2010, **39**, 4044–4056. (b) P. L. Holland, *Dalton Trans.*, 2010, **39**, 5415–5425.
- J. B. Geri, J. P. Shanahan and N. K. Szymczak, *J. Am. Chem. Soc.*, 2017, **139**, 5952–5956.
- S. Pietsch, E. C. Neeve, D. C. Apperley, R. Bertermann, F. Mo, D. Qiu, M. S. Cheung, L. Dang, J. Wang, U. Radius, Z. Lin, C. Kleeberg and T. B. Marder, *Chem. Eur. J.*, 2015, **21**, 7082–7098.
- J. D. Satterlee, *Concepts Magn. Reson.*, 1990, **2**, 69–79.
- (a) T. R. Dugan, X. Sun, E. V Rybak-Akimova, O. Olatunji-Ojo, T. R. Cundari and P. L. Holland, *J. Am. Chem. Soc.*, 2011, **133**, 12418–12421. (b) T. R. Dugan, J. M. Goldberg, W. W. Brennessel and P. L. Holland, *Organometallics*, 2012, **31**, 1349–1360.
- (a) N. Toriumi, K. Yamashita and N. Iwasawa, *Chem. Eur. J.*, 2021, **27**, 12635–12641. (b) Q. K. Kang, Y. Lin, Y. Li, L. Xu, K. Li and H. Shi, *Angew. Chem., Int. Ed.*, 2021, **60**, 20391–20399. (c) Y. Nakamura, N. Yoshikai, L. Ilies and E. Nakamura, *Org. Lett.*, 2012, **14**, 3316–3319. (d) Q.-K. Kang, Y. Lin, Y. Li, L. Xu, K. Li and H. Shi, *Angew. Chem., Int. Ed.*, 2021, **60**, 20391–20399. (e) D. Guijarro and M. Yus, *Tetrahedron*, 2000, **56**, 1135–1138.
- D.-G. Yu and Z.-J. Shi, *Angew. Chem., Int. Ed.*, 2011, **50**, 7097–7100.
- (a) E. Zars, L. Gravogl, M. Gau, P. J. Carroll, K. Meyer and D. J. Mindiola, *Inorg. Chem.*, 2022, **61**, 1079–1090. (b) D. Sorsche, M. E. Miehlich, E. M. Zolnhofer, P. J. Carroll, K. Meyer and D. J. Mindiola, *Inorg. Chem.*, 2018, **57**, 11552–11559.



### Data Availability Statement

Electronic Supplementary Information (ESI) available and contains complete experimental details and spectral data. All structural data is available in cif and cifcheck files, and have been deposited in the CCDC.

